Differential ranges and angular distributions of Ba fragments from the interaction of ^{238}U with 11.5-GeV protons

N. T. Porile, S. Pandian, H. Klonk, and C. R. Rudy

Department of Chemistry, Purdue University, W. Lafayette, Indiana 47907

E. P. Steinberg

Chemistry Division, Argonne National Laboratory, Argonne, Illinois 60439

(Received 28 August 1978)

Angular distributions and differential ranges at 90° to the beam direction have been measured for the following products from the interaction of ^{238}U with 11.5-GeV protons: ^{128}Ba, ^{131}La, ^{131}Ba (independent), ^{135}Ba^m, and ^{140}Ba. All the angular distributions peak at sideward angles. A two-parameter ($n_{\parallel}$ and b/a) fit to the angular distributions based on the two-step model yields an anisotropy parameter, b/a, of ~ -0.2 for all products. The value of $\langle v_{\parallel} \rangle$, the mean forward component of velocity of the struck nuclei, is also insensitive to the composition of the observed products. A sharp transition in the momentum spectra derived from the differential ranges is observed just over one Z unit to the neutron-deficient side of stability. Products on the neutron-rich side of this transition have narrow, symmetric spectra, with mean values of ~ 130 $(\text{MeV}A)^{1/2}$, that are characteristic of fission. Products on the neutron deficient side have broad, asymmetric spectra, with a mean value of only ~ 70 $(\text{MeV}A)^{1/2}$, as expected for a deep spallation mechanism. The spectrum of independently formed ^{131}Ba, which lies in the transition region, was decomposed into fission and deep spallation contributions, with the latter accounting for most of the cross section.

NUCLEAR REACTIONS ^{238}U(p, x) ^{128}Ba, ^{131}La, ^{131}Ba, ^{135}Ba^m, ^{140}Ba, $E_p = 11.5$ GeV; measured angular distributions and differential ranges at 90°; inferred momentum spectra.

I. INTRODUCTION

In a recent study of the interaction of ^{238}U with 11.5-GeV protons, Yu and Porile[1,2] measured the cross sections and recoil properties of eight isobaric nuclides with $A = 131$. This detailed study of isobaric behavior yielded a number of important results, which are best discussed with reference to Fig. 1, taken from this earlier work. It is seen that the ranges, and hence the kinetic energies, of the neutron-excessive and near neutron-deficient nuclides are high and are, in fact, consistent with a binary fission mechanism. The gentle, linear decrease of range with increasing fragment Z is primarily due to the fact that these products are formed in interactions in which an increasingly high excitation energy is transferred to the struck nucleus.[3] On the other hand, the ranges of the most neutron-deficient isobars are low and have been interpreted[4,5] in terms of a deep spallation process, involving the emission of both nucleons and light aggregates, as well as more massive fragments. The occurrence, at GeV energies, of a substantial difference between the ranges of neutron-deficient and neutron-excessive nuclides in the fission product mass region has been observed in a number of instances.[4-15] The concurrent mea-

surement of recoil properties and cross sections permitted Yu and Porile[1,2] to determine that the transition point between fission and deep spallation occurred well into the neutron-deficient hump of the isobaric yield distribution. The distribution depicted in Fig. 1 is in general agreement with the results obtained in a number of charge dispersion and isotopic yield distribution studies performed on $A \sim 120$–150 products from the interaction of ^{238}U with GeV protons.[16-21] However, while a double-peaked charge dispersion curve suggests the occurrence of two mechanisms, each characterized by a distinctive isobaric yield distribution, the combination of recoil and cross-section measurements indicates that the situation may be more complex.

In the present study we focus on the formation of ^{131}Ba and neighboring nuclides in the interaction of ^{238}U with 11.5-GeV protons. As shown in Fig. 1, the range of ^{131}Ba lies midway between the fission and deep spallation ranges. The most obvious explanation of this fact is that at $A = 131$ the transition between these processes occurs between $Z = 55$ and 57, with comparable contributions occurring at $Z = 56$. This explanation assumes that only two mechanisms are operative and this is far from certain. Starzyk and Sugarman[13] have thus postulated
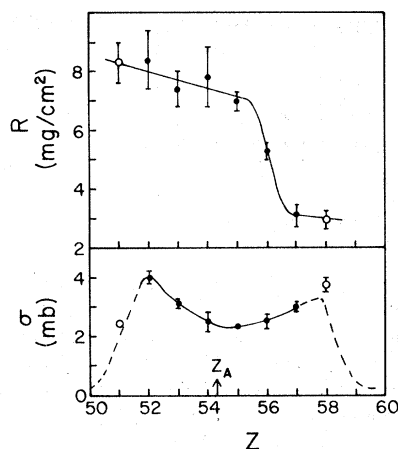
FIG. 1. Z dependence of the isobaric thick-target ranges (top panel) and cross sections (bottom) of $A = 131$ nuclides from the interaction of ^{238}U with 11.5-GeV protons. Closed points are independent products, open points cumulative products. The curve drawn through the cross sections represents the isobaric yield distribution; the dashed extensions are consistent with the plotted cumulative yields. The arrow indicates the value of Z_A at $A = 131$. Data taken from Refs. 1 and 2.

the occurrence of two types of fission, characterized by different ranges and contributing in different isobaric regions. Their novel high-deposition-energy process, referred to as Fission II, in fact makes its largest contribution at $A = 131$ in the vicinity of barium. Even if this process is not invoked, the mismatch between the Z values corresponding to the minimum in the isobaric yield distribution and to the drop in ranges indicates that more detailed studies of the range transition are needed before any definitive conclusions can be drawn about possible changes in mechanism.

We report here the results of differential range and angular distribution measurements performed on independently produced ^{131}Ba, its ^{131}La isobaric progenitor, and on several neighboring Ba nuclides. Similar data on some of these same products have been previously reported for 2.2-GeV incident protons.[9,12] At this lower energy the mechanism for the formation of neutron-deficient products is in the course of changing from fission to deep spallation.[4] The results presented here permit a determination of how the angular distribution and the width of the spectrum, quantities that cannot be inferred from thick-target recoil studies, change as the transition between mechanisms is achieved.

With respect to the formation of ^{131}Ba, the contribution from high- and low-range processes should be clearly visible in the differential range spectrum. Depending on the width of the curves one should thus obtain either a double-peaked range or a very broad distribution, resolvable in-

to two curves on the basis of the ranges of neighboring deep spallation and fission products. Furthermore, the angular distribution measurements at 2.2 GeV (Ref. 9) have shown that the curve obtained for ^{140}Ba peaks in the vicinity of 90° while that of cumulative ^{131}Ba is forward peaked. If this difference persists at 11.5 GeV, it thus might also be possible to unravel the contribution of two mechanisms to ^{131}Ba formation on the basis of the angular distribution.

II. EXPERIMENTAL

The irradiations were performed at the Argonne National Laboratory zero-gradient synchrotron (ZGS). The targets consisted of thin (100–300 $\mu g/cm^2$) UF_4 deposits evaporated onto high-purity 20 μm aluminum foil. These foils were mounted at 30° to the beam in a holder which was used for both the angular distribution and differential range measurements. The catcher foil holder consisted of a cylindrical bed facing the leading edge of the target from a distance of 5.1 cm. The catchers intercepted the angular range of 15°–105° relative to the beam direction and the assembly could be rotated to permit measurements at the corresponding backward angles. The differential range measurements were performed on fragments emitted at 75°–105° to the beam and this angular interval was defined by a mask placed over the catcher foils. Because of the low counting rates, the catcher foils subtended a large fraction of the available solid angle. The resulting mismatch between the spherical reaction coordinates and the cylindrical catcher angles dictated that the foils be cut along curves of constant recoil angle for a point source of recoils. The solid angles subtended by each catcher as well as the average recoil angles were evaluated with a code[22] which, in addition to the target-catcher geometry, took into account the beam profile at the target location. This profile was determined after bombardment by cutting the target into 12–20 small rectangles and assaying the ^{24}Na activity induced in the aluminum target backing. The details of the calculation as well as the relevant dimensions of the assembly have been published elsewhere.[23]

For the angular distribution measurements, the catchers consisted of two layers of 20 μm thick aluminum foil of high purity (99.999%). It was established that no Ba recoils penetrated into the second foil and the latter merely served to protect the catcher from any possible recoil products originating in the catcher bed. The catcher foils were cut into 15° wide strips. In the case of the differential range measurements the catchers consisted of a stack of 200–300 $\mu g/cm^2$ thick Mylar

foils[24] selected from batches with good uniformity. In a given stack, the variation in foil thickness was less than 3%.

The target-catcher assembly was irradiated for 30–45 min with 11.5-GeV protons in the internal beam of the ZGS. The holder was kept in a retracted position until each beam pulse attained this energy and was then flipped to expose the target to the beam. An aluminum beam bumper mounted next to the catcher holder served to protect the catchers from the beam.

The radiochemical procedure to which the foils were subjected after irradiation was designed to separate 11.5 day ^{131}Ba from its 59 min ^{131}La parent. The various catcher foils were dissolved and barium was quickly separated as $Ba(NO_3)_2$. The supernate was purified from any remaining barium by a second precipitation of this compound and was then allowed to stand for a minimum of 7 h to permit the complete decay of ^{131}La to ^{131}Ba. At this time additional barium carrier was added and $Ba(NO_3)_2$ precipitated. Both sets of Ba samples, those containing independently formed ^{131}Ba as well as the other Ba isotopes, and those containing ^{131}Ba from the decay of ^{131}La, were further purified by standard techniques.

The samples were assayed with Ge(Li) spectrometers. Results were obtained for the following nuclides on the basis of the γ rays listed in parentheses: ^{128}Ba(443 keV), ^{131}Ba(123, 496), ^{131}La(123, 496), ^{135}Ba^m(268), ^{140}Ba(537). While the chemical procedure did not specifically separate barium from radium, it was established in a separate experiment that the γ rays of interest were free from contamination due to radium isotopes or their radioactive decay products. The counting rates were in all cases corrected for radioactive decay and chemical yield in order to obtain the results of interest.

The data obtained for ^{131}Ba had, in addition, to be corrected for the decay of ^{131}La during irradiation and prior to the first Ba separation. This correction was applied on the basis of the ^{131}La data obtained in the same experiment as a given set of Ba results. One problem encountered in making this correction was that at the time of the Ba separation the parent of ^{131}La, 10 min ^{131}Ce, had not as yet completely decayed. Therefore, a correction based on the experimentally determined cumulative yield of ^{131}La overestimates the actual contribution of this nuclide to the observed ^{131}Ba activity. The incomplete decay of ^{131}Ce was taken into account on the assumption that the angular distribution and differential range of this nuclide are identical to those of ^{131}La, using the known[1] production cross sections of these nuclides to correct the magnitude of the ^{131}La activities. This

assumption is reasonable in view of the fact that the average ranges and forward-to-backward emission ratios of these nuclides are equal.[1] The correction to the ^{131}Ba activities obtained in this fashion amounted, on the average, to about 60%. If it had been assumed that all the ^{131}Ce had decayed to ^{131}La at the time of the Ba separation, the correction would have gone up to ~70%.

In order to ensure the validity of the results, two subsidiary experiments were performed. The possible contribution to the Ba activity from reactions occurring in the target holder or target backing material was investigated in a blank angular distribution experiment. An upper limit of 2% was set on extraneous sources of barium fragments. The Mylar foils used in the differential range experiments were also found to be free of impurities that could give rise to Ba nuclides by noting that no activity could be detected in the last two or three foils in the stack.

The possible effect of target thickness on the data was investigated by comparing the angular distributions obtained with 100 and 300 $\mu g/cm^2$ thick targets. No discernible difference could be detected and we conclude that scattering effects are negligible at these thicknesses. In a previous study of the differential ranges of Ba fragments from the interaction of uranium with 2.2-GeV protons,[9] broadening due to target thickness was observed for a 0.38 mg/cm^2 U target but not for a 0.17 mg/cm^2 U target. Since our UF$_4$ targets were closely comparable in effective thickness to the latter, we conclude that the range curves are also unaffected by scattering in the target.

III. RESULTS

A. Differential ranges

A typical set of range histograms is shown in Fig. 2. The uncertainties in the data are based on those in the thickness and uniformity of the foils (3%), chemical yield assays (2%), and disintegration rate determinations. At the peaks in the ranges, the latter were about 3% for all nuclides except ^{131}Ba, which had a 10% uncertainty from this source. The reason for this larger error is the sizable correction for the contribution from ^{131}La prior to separation. The fluctuations of the relative intensities in a given range spectrum are roughly consistent with these estimates.

The experimental curves required several corrections. Because of the significant thickness of the Mylar foils a resolution correction was needed, particularly for the narrow fission curves. The procedure was similar to that used in previous differential range studies[9,12] and amounted to a
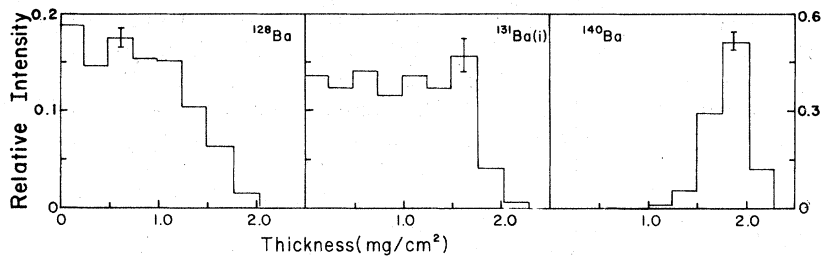
FIG. 2. Uncorrected differential ranges obtained at 90° to the beam of selected Ba nuclides from the interaction of ^{238}U with 11.5-GeV protons. Results are those of a typical experiment.

~10% reduction in the width of these curves. Two related corrections had to be applied on account of the large solid angle subtended by the catchers and the ensuing spread in the path length of recoiling fragments. The occurrence of these oblique paths increases the effective thickness of the catchers and target. The magnitude of these effects was calculated by an adaptation of the code written to evaluate the solid angles in the angular distribution experiments.[22] The program divided the catcher surface into ~1000 segments and the target into 20 segments and evaluated the path lengths of recoils originating at each of these target points and stopping in each catcher segment. The results were averaged over the target using the beam profile to provide the weighting factors, and over the catchers using the calculated solid angles subtended by each segment as weights. This calculation indicated that it was necessary to increase the thickness of each catcher foil by 6–7% and that of the target by ~25%. The target correction was actually due in about equal measure to the above effect and to the inclination of the target. It was assumed that, on the average, the fragments traversed half the corrected target thickness and the latter was converted to an equivalent Mylar thickness on the basis of the relative stopping powers of Mylar and UF_4 for barium fragments.[25] Since the ratio of stopping powers varies by only 20% over the entire range of fragment energies, an average value was used. As an example of this procedure, a target with an actual thickness of 200 μg/cm^2 corresponds to 36 μg/cm^2 Mylar.

The corrected differential ranges were converted to momentum and energy spectra by use of the range-energy tables of Northcliffe and Schilling.[25] For the cumulatively formed products the conversion was made on the basis of the effective Z values of these nuclides, Z_{eff}, obtained from the 11.5-GeV charge dispersion.[1] This quantity is defined as $Z_{eff} = \sum \sigma_i Z_i / \sum \sigma_i$ and is the average Z value of all nuclides contributing to a cumulatively formed product weighted by their respective cross sections. A small correction (0.2–1.7%) was ap-

plied to account for the difference between the tabulated path lengths and the experimentally determined projected ranges. The magnitude of this correction was obtained from the work of Lindhard, Scharff, and Schiøtt.[26]

The momentum spectra are displayed in Fig. 3 and the average ranges, energies, and momenta are tabulated in Table I in order of increasing $Z_A - Z_{eff}$, the distance from stability of the product in question expressed in Z units. Three or four separate experiments were performed for each nuclide and the resulting differential ranges were individually transformed to momenta. The results from the various experiments were normalized to each other by setting the total intensity equal to unity. The curves in Fig. 3 are hand-drawn through the weighted averages of the individual determinations, except in the case of ^{135}Ba^m and ^{140}Ba, where they are Gaussian fits. The standard deviations of the Gaussians are included in Table I.
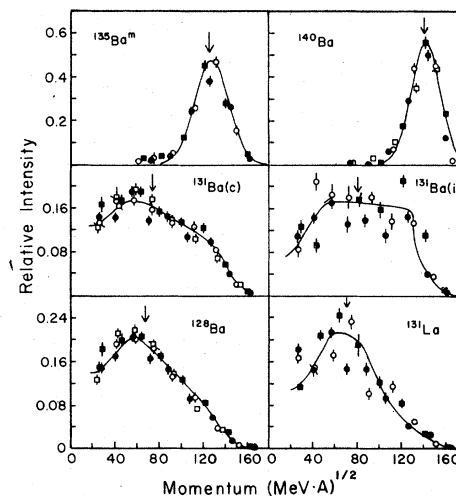

FIG. 3. Momentum spectra obtained at 90° to the beam. The various symbols represent the results of different experiments. The curves through the ^{140}Ba and ^{135}Ba^m data are Gaussian fits. The curves for the other nuclides are hand-drawn through the averages of the various experiments. The arrows surmounting the curves represent the mean momenta.

TABLE I. Average quantities obtained from differential range spectra of products from the interaction of ^{238}U with 11.5-GeV protons measured at 90° to the beam.

Nuclide	$Z_A - Z_{eff}$ [c]	$\bar{R}$ (mg/cm²)	$\bar{T}$ (MeV)	$\bar{P}$ [(MeV A)$^{1/2}$]	FWHM [(MeV A)$^{1/2}$]
^{128}Ba(c) [a]	−3.60	0.845 ± 0.006	22.1	68.2	110
^{131}La(c)	−3.60	0.880 ± 0.024	22.7	70.2	80
^{131}Ba(c)	−3.03	0.947 ± 0.007	26.0	74.4	130
^{131}Ba(i) [b]	−1.73	1.058 ± 0.017	30.0	80.6	130
^{135}Ba^m(i)	−0.40	1.741 ± 0.008	59.0	125 (15) [d]	35
^{140}Ba(c)	2.30	1.981 ± 0.009	71.1	140 (13) [d]	31

[a] Cumulatively formed product.
[b] Independently formed product.
[c] Z_{eff} is defined in the text.
[d] Standard deviation in the Gaussian fit.

The results obtained for most nuclides in the various experiments agree with each other within the estimated uncertainties. The most notable exceptions are ^{131}La and ^{131}Ba(i) (independent), for which considerable scatter occurs. This lack of reproducibility must reflect some additional uncertainties in the correction for the decay of ^{131}La to ^{131}Ba. The spectrum of cumulatively formed ^{131}Ba, denoted as ^{131}Ba(c), which is based on the sum of the disintegration rates of ^{131}La and ^{131}Ba thus shows much less scatter. The quantities listed in Table I are weighted averages, the experimental uncertainties in these values being 2–3%. In addition, we estimate a 5% uncertainty in the use of the range-energy relation.[25]

B. Angular distributions

The angular distributions were obtained from the disintegration rates by applying a correction for the solid angle intercepted by each foil using the code described above. The solid angles ranged from 0.16 sr at forward or backward angles to 0.34 sr at sideward angles. Four experiments were performed at forward angles and three at backward angles. Since the mean recoil angles corresponding to each catcher strip were virtually identical for the various experiments, the results for either forward or backward angles were averaged after the data were normalized to each other. The resulting distributions were combined by normalizing them at their common 75°–90° and 90°–105° intervals. Figure 4 shows the weighted average angular distributions as differential cross sections normalized to yield a value of 4π when integrated over all space. The error bars represent the larger of the estimated uncertainties in the individual determinations, which were at most comparable to those in the differential ranges, and the standard deviations in the mean values.

The angular distributions were fitted with an equation based on the two-step model commonly

invoked in the interpretation of high-energy reactions. Let $\vec{v}$ be the velocity acquired by the struck nucleus as a result of the initial interaction. The components of v along and at right angles to the beam direction are designated $v_{\parallel}$ and $v_{\perp}$, respectively. The mean velocity acquired by the fragment in the breakup step is denoted as $\vec{V}$ and its angular distribution in the moving frame is assumed to obey the relation

$$F(\theta) = \frac{1 + (b/a)\cos^2\theta}{1 + b/3a} , \qquad (1)$$

where b/a is the anisotropy parameter. The ratios $\eta_{\parallel} = v_{\parallel}/V$ and $\eta_{\perp} = v_{\perp}/V$, which are a measure of the relative velocities imparted in the two steps, are of interest. The laboratory angular distribution may be expressed in terms of $\eta_{\parallel}$ and b/a by the equation[27]
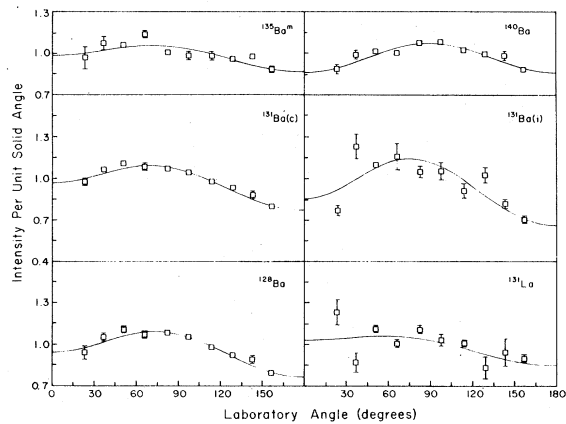

FIG. 4. Angular distributions in the laboratory system. The points are weighted averages of several determinations. The curves are based on Eq. (2).

$$F_L(\theta_L) = \frac{1 + (b/a)\cos^2[\theta_L + \sin^{-1}(\eta_\parallel \sin\theta_L)]}{1 + b/3a}$$

$$\times \frac{[\eta_\parallel \cos\theta_L + (1 - \eta_\parallel^2 \sin^2\theta_L)^{1/2}]^2}{(1 - \eta_\parallel^2 \sin^2\theta_L)^{1/2}}, \quad (2)$$

where $F_L(\theta_L)$ is the laboratory differential cross section at angle θ_L. The integral of F_L over θ_L is equal to 4π. This equation assumes that $\eta_\parallel < 1$ not only on the average, but for each interaction. The effect of overlapping distributions of $v_\parallel$ and V has been discussed elsewhere.[28] Equations for $F_L(\theta_L)$ which include terms in $\eta_\perp$ have been published or proposed.[29] The inclusion of $\eta_\perp$ complicates the analysis considerably and the equations are based on approximations which are problematic.[30] Since satisfactory fits to the data can be obtained with Eq. (2), we have neglected the effect of $\eta_\perp$.

The parameters obtained from a least squares fit of Eq. (2) to the data are summarized in Table II and the calculated angular distributions are shown as curves in Fig. 4. The curves fit the data quite well although, as in the case of the differential ranges, the results for ^{131}La and ^{131}Ba(i) show a good deal of scatter that disappears when these data are combined to yield the distribution of ^{131}Ba(c). Table II also includes the ratio of forward to backward emission F/B obtained by integrating the forward and backward halves of the fitted angular distribution over all space. The values of $\langle v_\parallel \rangle$, the mean value of the forward component of the velocity of the struck nucleus, may be obtained[9] from the relation $\langle v_\parallel \rangle = \eta_\parallel / \langle V^{-1} \rangle$, where $\langle V^{-1} \rangle$ was obtained from the differential range spectra. (We follow previous[9] usage and explicitly indicate that the velocities are average quantities.)

IV. DISCUSSION

A. Differential ranges and angular distributions

In this section we shall discuss the results of the two types of experiments in the light of the known properties of massive fragments produced in the interaction of uranium with multi-GeV protons.

The ranges of neutron-deficient nuclides ($Z_A - Z_{\text{eff}} < -2$) lying in the fission product mass region decrease by a factor of 2 and the values of F/B go through a maximum in the vicinity of 3 GeV and approach those of the neutron-excessive products at higher energies.[4] In contrast, fission continues to be the dominant mechanism for the formation of neutron-excessive products at multi-GeV energies and these nuclides have essentially the same high ranges and low F/B ratios as at lower energies. These data are indicative of a change in mechanism for the formation of neutron-deficient products in the vicinity of 3-GeV bombarding energy from binary fission to deep spallation.

In view of these observations, which were established in thick-target recoil studies, we expect the mean kinetic energies and momenta of the fragments to show a sharp discontinuity on the near neutron-deficient side of stability while the values of F/B should increase only slightly with increasing neutron deficiency. Thick-target recoil studies do not provide information on the width of the energy or momentum distributions or on the shape of the angular distributions. Our experiment provides the first results at 11.5 GeV on the variation of these quantities with composition.

Figure 5 shows the dependence on fragment composition of some of the quantities obtained in the present study. For comparison we have included, where appropriate, results on fragments in the mass region of interest from the 11.5-GeV thick-target experiment of Yu and Porile[1,2] as well as from the 2.2-GeV angular distribution and 90° differential range studies of Cumming and collaborators.[9,12]

The mean kinetic energies are seen to increase between $Z_A - Z_{\text{eff}}$ of −1.5 and −0.5 by a factor of 2, i.e., from 20–30 to 60–70 MeV. Our results are too sparse to permit an unambiguous determination of the variation of kinetic energy with composition on either side of the transition. The more complete results of Yu and Porile[1,2] on the neutron-rich side of the transition parallel the trend observed in the present work. However, the kinetic energies from the thick-target work are

TABLE II. Results of least squares two-parameter fit to angular distributions based on the two-step vector model.

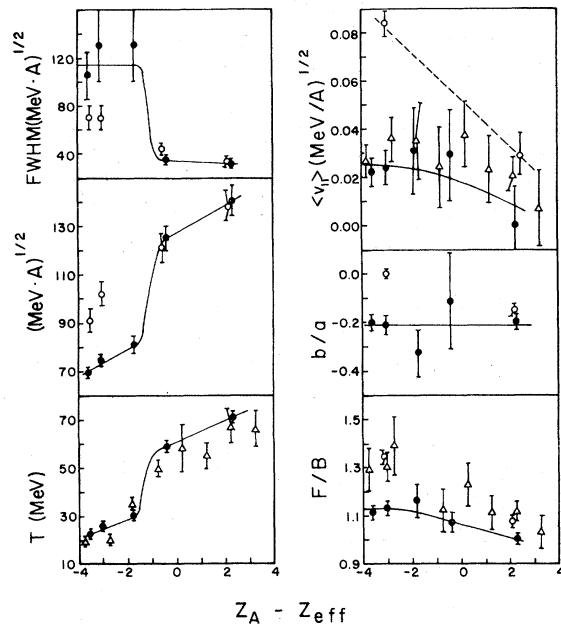| Nuclide	$\eta_\parallel$	b/a	F/B	$\langle v_\parallel \rangle$ [(MeV/A)$^{1/2}$]
^{128}Ba	0.052 ± 0.014	−0.207 ± 0.029	1.12 ± 0.02	0.022 ± 0.006
^{131}La	0.049 ± 0.041	−0.091 ± 0.137	1.11 ± 0.07	0.021 ± 0.018
^{131}Ba(c)	0.057 ± 0.016	−0.188 ± 0.040	1.13 ± 0.03	0.024 ± 0.007
^{131}Ba(i)	0.066 ± 0.038	−0.327 ± 0.108	1.16 ± 0.07	0.031 ± 0.018
^{135}Ba^m	0.033 ± 0.021	−0.114 ± 0.200	1.07 ± 0.04	0.029 ± 0.019
^{140}Ba	0.000 ± 0.015	−0.197 ± 0.028	1.00 ± 0.02	0.000 ± 0.016

$Z_A - Z_{eff}$

FIG. 5. Dependence of various quantities obtained from the spectra and angular distributions on fragment composition. Starting at the lower left corner and moving clockwise are the mean kinetic energy of the fragments, their mean momentum, the full width at half maximum of the momentum distributions, the mean forward component of velocity of the struck nucleus, the anisotropy parameter, and the ratio of forward to backward emission; ●, present work (the curves show the trend of these points); △, 11.5-GeV thick-target data (Refs. 1,2) ○, 2.2-GeV thin-target data (Refs. 9,12). See text for definition of Z_{eff}.

some 10% lower. This difference presumably reflects, in the main, that between the range-energy relations used in the two studies. On the neutron-deficient side of the transition, Yu and Porile[1] find less of a variation in kinetic energy with composition than is obtained in the present work. The kinetic energy baseline set by their most neutron-deficient products suggests that ^{131}Ba has comparable contributions from deep spallation and fission. An analysis of the ^{131}Ba results obtained in the present experiment is deferred to the following section.

The mean momenta display a behavior similar to that of the kinetic energies. Also shown are the values obtained for the same products at 2.2 GeV by Bächmann and Cumming.[12] On the neutron-rich side of the transition the two sets of results are in excellent agreement. This accord is an indication of the fact that the momentum of fission products remains essentially invariant at GeV bombarding energies. Cumming and Bächmann[5] have examined the systematics of high-energy fission

product momenta.[4,8,10,11] These momenta range between 125 and 140 $(\text{MeV}A)^{1/2}$ and are consistent with those of collinear or nearly collinear fission fragments detected in counter experiments performed at 2.9 GeV.[31] The present results are in accord with these systematics.

In contrast to the lack of energy dependence of the momentum of fission products, the momentum of the very neutron-deficient products is seen to be substantially higher at 2.2 than at 11.5 GeV. Beg and Porile[4] have shown that at 2 GeV the ranges of these products, and hence their momenta, are in the course of decreasing from the high values expected for a fission mechanism to the lower values characteristic of deep spallation. Cumming and collaborators[5,28] have systematized the momenta of deep spallation products by developing a simple model which attributes the fragment momentum to the random addition of the momenta of the emitted particles. These workers[5] derived an equation relating the mean kinetic energy of the emitted particles to the mass difference between target and product, ΔA. This energy increases slowly with ΔA and for $\Delta A = 110$ is ~45 MeV. Since the ranges of the products in question appear to level off by 11.5 GeV, these systematics should be applicable to the present data. Our results for ^{128}Ba and ^{131}La lead to a mean kinetic energy of 48 MeV, in reasonably good agreement with the Cumming systematics.

The widths of the momentum distributions display the opposite dependence on composition as the mean values; products having high momenta have narrow distributions and viceversa. This difference, which has been seen before,[9] is a natural consequence of the kinematics of fission and deep spallation. Figure 5 shows that the widths of the momentum spectra of the fission products are the same at 2.2 as at 11.5 GeV. On the other hand, the widths of the spectra of neutron-deficient products are substantially narrower at the lower energy. Once again, this is an indication of the transition from fission to deep spallation that occurs at this lower energy. Crespo, Cumming, and Poskanzer[9] have inferred the momentum spectrum of neutron-deficient barium fragments produced from uranium in deep spallation by scaling the spectrum of ^{149}Tb emitted at 90° in the interaction of gold with 2.2-GeV protons.[28] Their inferred spectrum peaks at just under 50 $(\text{MeV}A)^{1/2}$ and has a full width at half maximum of about 60 $(\text{MeV}A)^{1/2}$. These workers estimated an 18% contribution of deep spallation to cumulatively formed ^{131}Ba on the basis of this spectrum. The deep spallation spectra displayed in Fig. 3 peak at about 60 $(\text{MeV}A)^{1/2}$ and have a width of at least 100 $(\text{MeV}A)^{1/2}$. The use of this broader distribution

would increase the estimated magnitude of the deep spallation contribution at 2.2 GeV on the assumption that the deep spallation spectrum is independent of bombarding energy.

The values of F/B exhibit a slight decrease with increasing $Z_A - Z_{eff}$. The thick-target F/B obtained at 11.5 GeV track the behavior of the thin-target values but are higher. This difference has no profound significance and is merely a consequence of the different relation between F/B and the velocity vectors for thick- and thin-target configurations.[32] The F/B of ^{131}Ba obtained in the thin-target experiment at 2.2 GeV (Ref. 9) is substantially higher than the present value. This is not surprising in view of the fact that the thick-target F/B attain their peak values at 3 GeV.[4]

The value of the anisotropy parameter b/a is approximately −0.2, independent of composition. Within the framework of a two-parameter fit to the two-step model, all fragments are preferentially emitted at sideward angles in the moving system. The situation is significantly different at 2.2 GeV. While b/a of ^{140}Ba, a fission product, is essentially the same as at 11.5 GeV, that of cumulatively formed ^{131}Ba is zero, indicating isotropy in the moving system. The combination of a relatively large $\eta_{\parallel}$ and zero b/a at 2.2 GeV leads to an angular distribution that is forward peaked in the laboratory system, while that of small $\eta_{\parallel}$ and negative b/a at 11.5 GeV leads to the observed sideward peaking. This type of change has been previously observed for light fragments[33,34] $(A \sim 20-50)$ but this is the first indication that a similar change occurs for deep spallation products. It is interesting to note that this transition is accompanied in all cases by F/B values that peak in the vicinity of 3 GeV,[4,35,36] although the precise energy at which the angular distributions change from forward- to sideward-peaked remains to be established. On the other hand, those products that do not exhibit a peak in F/B have angular distributions that do not change between 2 and 11 GeV. A number of possible causes of the change in the angular distributions have been considered.[33,34] While it seems likely that the observed effect is connected with the changes in the nature of proton-nucleus interactions at high energies,[37] a quantitative explanation has not as yet been given.

The last quantity to be discussed is the mean value of the forward component of velocity of the struck nucleus, $\langle v_{\parallel} \rangle$, plotted at the top right of Fig. 5. This quantity shows, at most, a slight decrease with increasing $Z_A - Z_{eff}$, a trend that is also shown by the thick-target recoil data. The results obtained at 2.2 GeV show a totally different behavior. It is seen that the $\langle v_{\parallel} \rangle$ associated with the production of neutron-deficient products

is much higher than at 11.5 GeV while that associated with the formation of neutron-excessive nuclides is nearly the same at the two energies. The trend displayed by the 2.2 GeV data is, in fact, that expected according to the two-step model of high-energy reactions. It is a well established fact that the forward component of velocity or momentum of the struck nucleus gives a measure of the average excitation energy $\bar{E}*$ transferred to it by the intranuclear cascade. This relation was first established[38,39] on the basis of the Metropolis cascade code,[40] was confirmed by the Vegas code,[41] and has most recently been derived[42] from the Bertini code[43] at 3 GeV. The variation of $\langle v_{\parallel} \rangle$ with composition at 2.2 GeV thus is an indication that $\bar{E}*$ of the residual nuclei leading to the observed products increases as the latter become more neutron deficient. This relation between excitation energy and fragment composition has been thoroughly established in experiments performed with 450-MeV protons[3,44,45] and primarily reflects the fact that the formation of neutron-deficient products from uranium requires the emission of more neutrons, and hence higher energies, than that of neutron-excessive products. The much weaker variation of $\langle v_{\parallel} \rangle$ with $Z_A - Z_{eff}$ obtained at 11.5 GeV thus may be an indication that the $\langle v_{\parallel} \rangle - \bar{E}*$ relation obtained up to 3 GeV ceases to be valid at higher energies. It has been suggested[34,42] that a possible change at this energy in the nature of the excitons from predominantly particles to holes could be the cause of a change in this relation. Alternatively, the two-step model, in which the intermediate nuclei can be characterized by $\langle v_{\parallel} \rangle$ and $\bar{E}*$ values, may not be applicable to deep spallation reactions. The emission of light fragments, which may be the partners of deep spallation products, cannot be completely accounted for by a two-step process at 3–6 GeV,[46,47] but, at least at 2.2 GeV, the formation of ^{131}Ba from uranium is consistent with such a mechanism.[9]

The preceding discussion of the dependence of various properties of products on their composition can be summarized succinctly: At bombarding energies below ~3 GeV neutron-deficient $(Z_A - Z \lesssim -2)$ and neutron-excessive (actually $Z_A - Z > -1$) products differ in those properties associated with the cascade step, i.e., $\langle v_{\parallel} \rangle$ and b/a. (Note that we associate b/a with the cascade even though it refers to the anisotropy of the breakup velocity. There is considerable evidence that b/a is actually determined by the angular momentum imparted in the cascade step.[9,48]) On the other hand, the properties determined by the second, or breakup, step, i.e., the energy or momentum spectra, are rather similar for both types of products. The opposite holds true at high (11.5 GeV) energies.

Now both types of products have essentially the same values of $\langle v_{\|} \rangle$ and b/a but drastically different energy spectra. This change in behavior is entirely due to the change in the mechanism of formation of the neutron-deficient products.

B. Contribution of deep spallation and fission to ^{131}Ba

As indicated in the Introduction, the present study was partly motivated by the indication, obtained from thick-target recoil studies,[1] that ^{131}Ba had comparable contributions from deep spallation and fission. This raised the possibility that either the spectrum or angular distribution could be resolved into distinctive components associated with each of these processes. The discussion in the preceding section has made it clear that the angular distributions of deep spallation and fission products are virtually identical at 11.5 GeV. Furthermore, in spite of the large difference in the mean momentum of these two types of products, the spectrum of ^{131}Ba, displayed in Fig. 3, is not resolvable into two components. While this may be due, in part, to the scatter in the data, it more fundamentally reflects the width of the deep spallation spectrum. It has already been mentioned that this spectrum peaks at ~60 $(\mathrm{MeV}\,A)^{1/2}$ and has a width of at least 100 $(\mathrm{MeV}\,A)^{1/2}$. This makes it difficult to resolve it from the fission peak, which is centered at 120–140 $(\mathrm{MeV}\,A)^{1/2}$ and has a width of 30–40 $(\mathrm{MeV}\,A)^{1/2}$.

In view of this difficulty we are forced to resort to the somewhat less satisfactory, but still valid, procedure of resolving the ^{131}Ba spectrum on the basis of the presently obtained spectra of fission and deep spallation products. The spectrum of ^{131}Ba expected for a fission mechanism may be obtained from the ^{140}Ba and ^{135}Ba^m spectra. As shown in Fig. 3, these spectra are very well fitted by Gaussians. The parameters of the fit are summarized in Table I. It is seen that the peak momentum decreases and the standard deviation increases with increasing neutron deficiency. These trends are a reflection of the higher excitation energy needed to produce less neutron-rich fission products. The higher excitation energy in turn leads to a greater mass loss and a larger spread of fissioning nuclei and thus to the lower magnitude and greater dispersion of the momentum. Similar results have been previously obtained at lower energies.[3,9] It thus seems reasonable to extrapolate the ^{140}Ba and ^{135}Ba^m parameters to the $Z_A - Z_{\mathrm{eff}}$ value of ^{131}Ba. We have performed a linear extrapolation but, in view of the small difference in the distance from stability, a different type of extrapolation would not materially affect the results. The Gaussian expected for the formation of ^{131}Ba

by fission is shown in Fig. 6.

The systematics of deep spallation products developed by Cumming and collaborators[5,30] suggest that the mean momentum and width of the distribution should increase with the target-product mass difference. It would therefore be most appropriate to use the ^{131}La spectrum as a measure of the deep spallation contribution to ^{131}Ba. However, as indicated in Fig. 3, the spectrum of ^{131}La has considerably more scatter than that of ^{128}Ba. We have therefore combined all the data for these two nuclides and used a curve hand-drawn through their weighted average values to represent the deep spallation spectrum.

We have fitted the ^{131}Ba spectrum with these two curves by adjusting their relative intensities so as to minimize the sum of the squares of the deviations from the curve drawn through the ^{131}Ba points. The results of this procedure are displayed in Fig. 6, which shows the deep spallation and fission curves, the sum curve, and the experimental points. The best fit corresponds to a $(25 \pm 16)\%$ contribution of fission. The large uncertainty in this value is primarily due to the scatter in the data points. Although this result is based on recoils emitted at 75°–105° to the beam, it can be taken as representative of all ^{131}Ba fragments because of the close similarity of the angular distributions of both fission and deep spallation products.
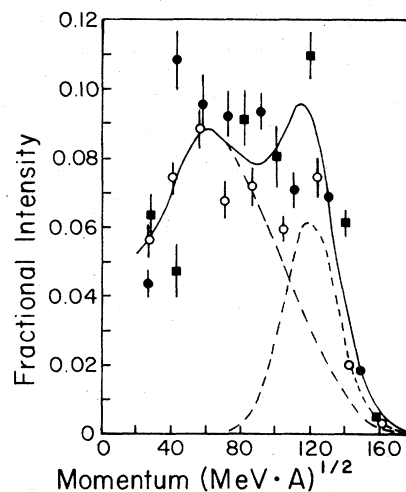

FIG. 6. Decomposition of the ^{131}Ba momentum spectrum into deep spallation and fission components. The dashed curves represent the component spectra adjusted in intensity to give the best fit and the solid curve is their sum. The points represent experimental values, with different symbols corresponding to different irradiations.

While the present study indicates that the fission contribution to ^{131}Ba formation is lower than that suggested by the data of Yu and Porile,[1,2] the results of these two studies appear to be consistent within the limits of error. Our results show that in the $A \sim 131$ mass region the transition from fission to deep spallation is centered at just over one Z unit to the neutron-deficient side of stability and is completed within less than two Z units. The location of this transition has been independently examined by Cumming and Bächmann[5] and Starzyk and Sugarman[13] on the basis of thick-target recoil data obtained above 10 GeV for products in the $A = 115-135$ and $A = 120-165$ mass regions, respectively. Both studies indicate that the transition occurs within less than two Z units and is centered at $Z_A - Z_{eff}$ of ~ -1.5. As shown in the present study, products in this mass region located at such a distance from stability can be expected to show contributions from both processes.

V. CONCLUSIONS

Differential range and angular distribution measurements performed on products in the $A \sim 130$ mass region from the interaction of ^{238}U with 11.5-GeV protons reveal some important similarities and differences between neutron-excessive and neutron-deficient products. All the angular distributions peak at sideward angles. A parametrization of the angular distributions based on the two-step model, in which the parameters to be derived from the fit are b/a and $\eta_\parallel$, yields b/a values of approximately -0.2 for both types of products. The values of $\langle v_\parallel \rangle$, the mean forward component of velocity transferred to the struck nuclei by the initial interaction, are also rather insensitive to composition. By contrast, the momentum or energy spectra of these two types of products differ widely. Neutron-excessive fragments have a mean momentum of ~ 130 $(MeV A)^{1/2}$

and the spectra are narrow and symmetric, with a full width of ~ 30 $(MeV A)^{1/2}$. On the other hand, neutron-deficient fragments have very broad [full width ~ 100 $(MeV A)^{1/2}$] and asymmetric spectra and their mean momentum is only about 70 $(MeV A)^{1/2}$. This difference is ascribed to one in reaction mechanisms. Neutron excessive products are formed in fission while neutron-deficient nuclides result from deep spallation. The change in mechanisms actually does not occur at stability but is centered just over one Z unit to the neutron-deficient side of Z_A. The transition is rather abrupt and occurs over less than two Z. The momentum spectrum of independent ^{131}Ba, which lies in this transition region, exhibits contributions from both mechanisms and a deconvolution procedure indicates that deep spallation accounts for most of the cross section.

Our results contrast with those previously obtained at 2.2 GeV.[9,12] At this lower energy the neutron-deficient fragments are primarily formed by fission involving the transfer of high excitation energies to the struck nuclei. As a result, the momentum spectra are not as different from those of the neutron-excessive products as at 11.5 GeV. On the other hand, those properties commonly associated with the initial interaction, i.e., $\langle v_\parallel \rangle$ and b/a, are strikingly different for the two types of products, reflecting the close connection at energies up to a few GeV between the linear and angular momentum of the residual nuclei and their excitation energy.

[1]Y. W. Yu and N. T. Porile, Phys. Rev. C **7**, 1597 (1973).

[2]Y. W. Yu, N. T. Porile, R. Warasila, and O. A. Schaeffer, Phys. Rev. C **8**, 1091 (1973).

[3]J. J. Hogan and N. Sugarman, Phys. Rev. **182**, 1210 (1969).

[4]K. Beg and N. T. Porile, Phys. Rev. C **3**, 1631 (1971).

[5]J. B. Cumming and K. Bächmann, Phys. Rev. C **6**, 1362 (1972).

[6]N. Sugarman, M. Campos, and K. Wielgoz, Phys. Rev. **101**, 388 (1956).

[7]J. Alexander, C. Baltzinger, and M. F. Gadzik, Phys. Rev. **129**, 1826 (1963).

[8]R. Brandt, in *Proceedings of the Symposium on the Physics and Chemistry of Fission, Salzburg, 1965*

(International Atomic Energy Agency, Vienna, 1965), Vol. II, p. 329.

[9]V. P. Crespo, J. B. Cumming, and A. M. Poskanzer, Phys. Rev. **174**, 1455 (1968).

[10]E. Hagebø and M. Ravn, J. Inorg. Nucl. Chem. **31**, 2649 (1969).

[11]J. A. Panontin and N. T. Porile, J. Inorg. Nucl. Chem. **32**, 1775 (1970).

[12]K. Bächmann and J. B. Cumming, Phys. Rev. C **5**, 210 (1972).

[13]P. M. Starzyk and N. Sugarman, Phys. Rev. C **8**, 1448 (1973).

[14]S. K. Chang and N. Sugarman, Phys. Rev. C **9**, 1138 (1974).

[15]Y. W. Yu and N. T. Porile, Phys. Rev. C 10, 167 (1974).

[16]G. Friedlander, L. Friedman, B. Gordon, and L. Yaffe, Phys. Rev. 129, 1809 (1963).

[17]G. Rudstam and G. Sørensen, J. Inorg. Nucl. Chem. 28, 771 (1966).

[18]E. Hagebø, J. Inorg. Nucl. Chem. 29, 2515 (1967).

[19]J. Chaumont, Ph.D. thesis, Université de Paris, 1970 (unpublished).

[20]K. Bächmann, J. Inorg. Nucl. Chem. 32, 1 (1970).

[21]Y. Y. Chu, E. M. Franz, G. Friedlander, and P. J. Karol, Phys. Rev. C 4, 2202 (1971).

[22]D. R. Fortney (unpublished).

[23]C. R. Rudy, N. T. Porile, and S. B. Kaufman, Nucl. Instrum. Methods 138, 19 (1976).

[24]We are grateful to the Plastic Products and Resins Department of Du Pont for providing us with this material.

[25]L. C. Northcliffe and R. F. Schilling, Nucl. Data A 7, 233 (1970).

[26]J. Lindhard, M. Scharff, and M. E. Schiøtt, K. Dan. Videnskab. Selsk. Mat.-Fys. Medd. 33, No. 14 (1963).

[27]J. B. Marion, T. I. Arnette, and H. C. Owens, Oak Ridge National Laboratory Report No. ORNL-2574, 1959 (unpublished).

[28]N. T. Porile, Phys. Rev. 185, 1371 (1969); V. P. Crespo, J. B. Cumming, and J. M. Alexander, Phys. Rev. C 2, 1777 (1970); L. Winsberg, Nucl. Instrum. 150, 1465 (1978).

[29]A. M. Poskanzer, J. B. Cumming, and R. Wolfgang, Phys. Rev. 129, 374 (1963); N. Sugarman (private communication).

[30]J. B. Cumming (private communication).

[31]L. P. Remsberg, F. Plasil, J. B. Cumming, and M. L. Perlman, Phys. Rev. 187, 1597 (1969).

[32]L. Winsberg and J. M. Alexander, in Nuclear Chem-istry, edited by L. Yaffe (Academic, New York, 1968), Vol. I, p. 340.

[33]L. P. Remsberg and D. G. Perry, Phys. Rev. Lett. 35, 361 (1975).

[34]D. R. Fortney and N. T. Porile, Phys. Lett. 76B, 553 (1978).

[35]S. B. Kaufman and M. W. Weisfield, Phys. Rev. C 11, 1258 (1975).

[36]Ø. Scheideman and N. T. Porile, Phys. Rev. C 14, 1534 (1976).

[37]W. Busza, in Proceedings of the VIIth International Colloquium on Multiparticle Reactions, Tutzing, Germany, 1976, edited by J. Bencke et al. (Max Planck Institute, Munich, 1976).

[38]N. T. Porile and N. Sugarman, Phys. Rev. 107, 1410 (1957).

[39]N. T. Porile, Phys. Rev. 120, 572 (1960).

[40]N. Metropolis, R. Bivins, M. Storm, A. Turkevich, J. M. Miller, and G. Friedlander, Phys. Rev. 110, 185 (1958).

[41]K. Chen, Z. Fraenkel, G. Friedlander, J. R. Grover, J. M. Miller, and Y. Shimamoto, Phys. Rev. 166, 949 (1968).

[42]S. B. Kaufman, E. P. Steinberg, and M. W. Weisfield, Phys. Rev. C 18, 1349 (1978).

[43]H. W. Bertini, Phys. Rev. C 6, 631 (1972).

[44]N. Sugarman, H. Munzel, J. A. Panontin, K. Wielgoz, M. V. Ramanaiah, G. Lange, and E. Lopez-Menchero, Phys. Rev. 143, 952 (1966).

[45]J. A. Panontin and N. T. Porile, J. Inorg. Nucl. Chem. 30, 2027 (1968).

[46]J. B. Cumming, R. J. Cross, Jr., J. Hudis, and A. M. Poskanzer, Phys. Rev. 134, B167 (1964).

[47]A. M. Poskanzer, G. W. Butler, and E. K. Hyde, Phys. Rev. C 3, 882 (1971).

[48]I. Halpern, Nucl. Phys. 11, 522 (1959).